ORGANOMETALLICS

Article

pubs.acs.org/Organometallics

Ligand Steric and Electronic Effects on β-Ketiminato Neutral Nickel(II) Olefin Polymerization Catalysts

Dong-Po Song,[†,‡] Xin-Cui Shi,[†,‡] Yong-Xia Wang,[†] Ji-Xing Yang,[†,‡] and Yue-Sheng Li*[,†]

[†]State Key Laboratory of Polymer Physics and Chemistry, Changchun Institute of Applied Chemistry, Chinese Academy of Sciences, Changchun 130022, People's Republic of China

[‡]Graduate School of the Chinese Academy of Sciences, Changchun Branch, Changchun 130023, People's Republic of China

Supporting Information

ABSTRACT: A series of novel neutral nickel complexes **3a−g** and **4a−d** bearing the β-ketiminato ligands [(2,6-$^{i}Pr_2C_6H_3$)N═CHCHC(R)O]Ni(R′)(L) (for **3a−g**, R′ = Me, L = Py, and R = ^{t}Bu (**3a**), Ph (**3b**), 1-naphthyl (**3c**), 9-anthryl (**3d**), PhNMe$_2$(*p*) (**3e**), PhOMe(*p*) (**3f**), PhCF$_3$(*p*) (**3g**); for **4a−d**, R′ = Ph, L = PPh$_3$, and ^{t}Bu (**4a**), Ph (**4b**), 1-naphthyl (**4c**), 9-anthryl (**4d**)) have been synthesized and characterized. The molecular structures of **3b−d,f,g** and **4a,c** were further confirmed by X-ray crystallographic analysis. These complexes were employed in ethylene polymerization to systematically investigate ligand steric and electronic effects on the catalytic properties, including activity, molecular weight (MW), and branching number of the polyethylene obtained. The complexes bearing more bulky ligands showed higher activities and produced more branched polyethylene. Electron-deficient ligands were found to increase the catalytic activity, decrease the MW, and enhance the branching content of the polyethylene. In addition, phosphine Ni^{II}−Ph complexes **4a−d** proved to be more active than the corresponding pyridine Ni^{II}−Me complexes **3a−d**, probably due to the easier dissociation of PPh$_3$ relative to a pyridine from a nickel center.

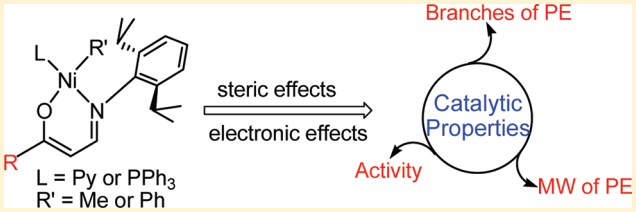

INTRODUCTION

The discovery of cationic Ni(II) and Pd(II) catalysts by Brookhart triggered a true exploration of the late-transition-metal catalysts for olefin polymerization.[1−7] The key feature of these catalysts lies in the bulky α-diimine ligand that has steric hindrance in the axial direction of the metal coordination plane to suppress the associative chain transfer.[1b] As a result, they showed outstanding performances in catalyzing ethylene polymerization and the copolymerization of olefin with polar monomers for production of functional polymers.[2] In the following years, more and more investigations have focused on the improvement of the catalytic properties through modification of the catalyst structure.[3−7] For example, Guan et al. reported the ligand electronic and steric effects on late-metal olefin polymerization catalysts **A** and **B** (see Scheme 1), which showed greatly improved catalytic performances in olefin (co)polymerization.[3] Recently, a series of C_2-symmetric late-metal catalysts **C** and **D** based on α-diimine ligands (see Scheme 1) were successfully prepared and employed in the living polymerization of ethylene, propylene, higher α-olefins, 4-alkylcyclopentene, etc.[6] Moreover, neutral palladium catalysts with phosphine−sulfonate ligands proved to be a success in the coordination−insertion copolymerization of ethylene with polar monomers after the first report by Drent et al.[8a] The sulfonate group, being a rather poor electron donor, was thought to be mainly responsible for the result.[9]

As early as the 1970s, the κ^2-[P,O]Ni catalysts **E** (see Scheme 2) discovered by Keim were the first examples of

Scheme 1. Modifications on the α-Diimine Ligand Backbone

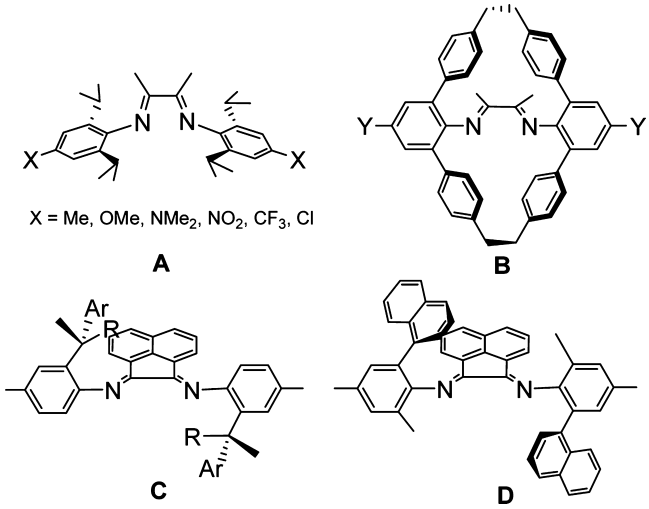

neutral nickel catalysts for the oligomerization of ethylene as practiced in Shell's higher olefin process (SHOP).[10] However, there was no significant progress in neutral nickel catalysts during the following two decades. At the beginning of the century, another breakthrough facilitating forays into neutral

Received: October 21, 2011
Published: January 20, 2012

   dx.doi.org/10.1021/om2010194 | *Organometallics* 2012, 31, 966−975

Scheme 2. Typical Neutral Nickel Complexes Reported Previously

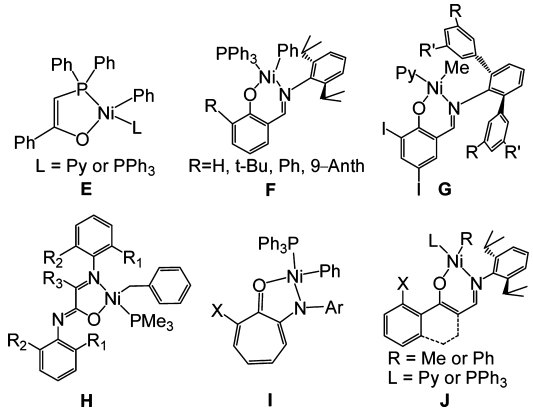

nickel catalysts came from Grubbs' research work with the discovery of salicylaldiminato catalysts **F** (see Scheme 2).[11] As a result, a majority of the investigations on neutral nickel catalysts have focused on salicylaldiminato ligand based species because of the facility for introducing various substituents on the backbone to enhance the activity and control the microstructure of the polymer.[12−16] For instance, the nickel salicylaldiminato methyl pyridine catalysts **G** (see Scheme 2) reported by Mecking's group, bearing substituted aryls at the 2,6-positions of the N-aryl moiety, displayed high efficiency for ethylene (co)polymerization in common solvents or unconventional media such as water and supercritical carbon dioxide.[12,13] Our group developed a series of nickel salicylaldiminato catalysts highly active toward olefin polymerization.[14] Marks et al. reported a bimetallic neutral nickel complex that showed a visible bimetallic association effect in ethylene polymerization and copolymerization with polar monomers.[15]

In addition to the neutral nickel salicylaldiminato complexes, complexes based on other ligand backbones were also developed by many research groups. As shown in Scheme 2, Bazan's group investigated various α-iminocarboxamide nickel catalysts **H**, which exhibited excellent performance in promoting olefin polymerization.[17] Brookhart et al. reported a series of neutral nickel catalysts containing five-membered nickel chelates (complexes **I** in Scheme 2) that exhibited high activities toward ethylene polymerization.[18] Brookhart and Mecking demonstrated that electron-poor neutral nickel enolatoimine catalysts were highly active for ethylene polymerization under nonaqueous or aqueous conditions.[19] All the modifications, namely ligand steric or electronic effects, on various ligand backbones have showed great influences on the catalytic performances of the olefin polymerization catalysts.

Recently, our group found the β-ketiminato ligand backbone promising for development of high-performance neutral nickel catalysts for olefin polymerization.[20] Modifications of the ligand structure (complexes **J** in Scheme 2), such as conjugation degree adjustment and geometric fixation, proved to be effective strategies to improve catalytic properties.[20c,d] However, the most important ligand-designing parameters, steric and electronic factors, were not completely involved in our previous reports. In this work, we aim to present a systematic investigation of both the steric and electronic effects of the β-ketiminato ligand on nickel(II) olefin polymerization catalysts. Interestingly, variation of the substituted R group (see Schemes 3 and 4) could greatly affect the catalytic properties, including

Scheme 3. General Synthetic Route of Nickel Complexes 3a−h

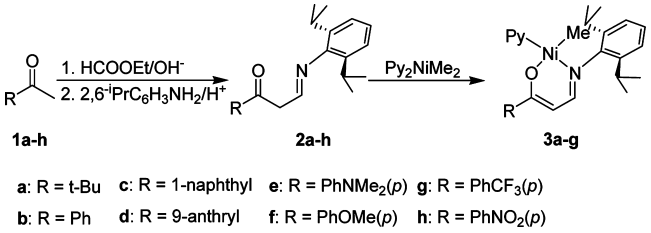

Scheme 4. General Synthetic Route of Nickel Complexes 4a−d

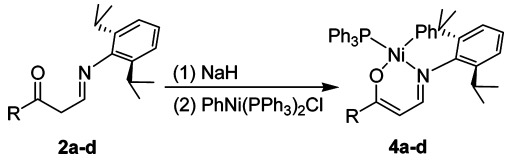

activity, molecular weight, and branching content of the polymer obtained.

RESULTS AND DISCUSSION

Synthesis and Characterization of β-Ketiminato Ligand Compounds. Scheme 3 illustrates the general synthetic route for β-ketiminato ligand compounds **2a−h** used in this study. First, β-diketones were prepared via the reaction between ethyl formate and the corresponding ketones with the help of a strong base such as potassium *tert*-butoxide. At the end of the reaction, a large amount of solid suspension was formed and was separated by filtration. Next, formic acid in ethanol was added to the solid until pH <7, affording the corresponding β-diketones. Finally, the β-diketones were used directly in the preparation of β-ketimines **2a,c−g** in good yields by the condensation reaction with 2,6-diisopropylaniline in ethanol containing a small amount of formic acid as a catalyst. The facile synthesis of compound **2b** has been reported in our previous publication.[20d] However, compound **2h** was synthesized in low yield, probably due to the strongly electron-withdrawing properties of the NO_2 group in a para position.

Compounds **2a−h** have been clearly characterized by ^{1}H and ^{13}C NMR spectra. The chemical shifts from 11.4 to 11.9 ppm in ^{1}H NMR are the characteristic signals for the N−H of the ligand compound, and the chemical shifts in the downfield region of ^{13}C NMR spectra (187−191 ppm) are the corresponding peaks for the carbons connected to nitrogens (N=C). For compounds **2e−h**, variation of the substituent at the para position leads to visible electronic effects on the ligand backbone. As shown in Figure 1, the chemical shift for N−H increases in the sequence NMe_2 < OMe < H < CF_3 < NO_2, which correlates strongly with the para Hammett substituent constant σ_p of these substituted groups on the ligands.[21] This can be explained by the fact that electron-withdrawing groups, such as CF_3 and NO_2, would reduce the electron density of the ligand backbone, resulting in a more reactive hydrogen on the nitrogen atom. In addition, the N=C signals in ^{13}C NMR for compounds **2g,h** with electron-withdrawing groups (CF_3, NO_2) shift to the upfield region relative to compounds **2e,f** with electron-donating substituents (OMe, NMe_2), which provides further evidence for the electronic effects. Such modulation of electronic density on the ligand backbone would subsequently

dx.doi.org/10.1021/om2010194 | *Organometallics* 2012, 31, 966−975

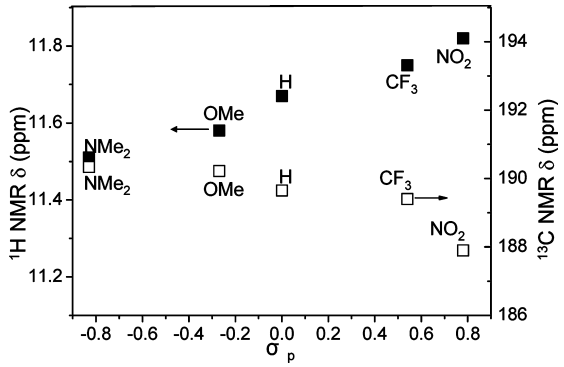

Figure 1. Chemical shifts (ppm) for N−H in ^{1}H NMR (left) and N=C in ^{13}C NMR (right) of compounds **2b** and **2e**−**h** versus the para Hammett substituent constant σ_p.[21]

influence the electron environment of the nickel(II) centers of our target complexes and thus their catalytic performances (vide infra).

Synthesis and Characterization of Neutral β-Ketiminato Nickel Complexes. According to the literature,[12c] β-ketiminato pyridine Ni^{II}−Me complexes **3a**,**c**−**g** were successfully prepared in high yields (more than 90%) by adding (pyridine)$_2$NiMe$_2$ to toluene solutions of ligands **5a**−**c** with vigorous stirring (Scheme 3). At first, the reaction systems were cooled to about −30 °C and then warmed to room temperature. The facile synthesis of complex **3b** has been reported in our previous publication.[20d] Unfortunately, our attempt to synthesize complex **3h** was a complete failure, probably due to the strongly electron-withdrawing group (NO$_2$) at the para position. In order to confirm the possible influence of the electronic substituent, natural population analysis (NPA) was subsequently performed to evaluate the substituted effects on the electron environment of the nickel(II) centers for complexes **3b**,**e**−**h** with electron-donating or electron-withdrawing groups,[22] and the calculated results are shown in Figure 2. Although the synthesis of complex **3h** was

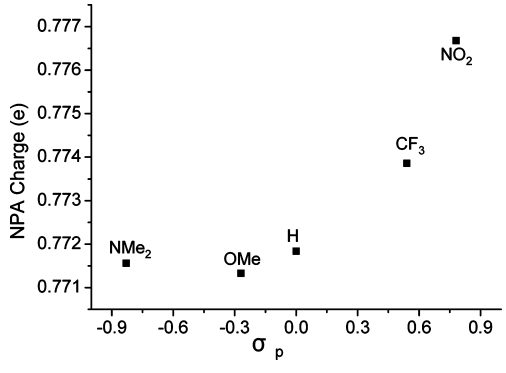

Figure 2. NPA charge on nickel(II) centers for catalysts **3e** (NMe$_2$), **3f** (OMe), **3b** (H), **3g** (CF$_3$), and **3h** (NO$_2$) versus the para Hammett substituent constant σ_p.[21]

not successful, we carried out the calculation to find out the large difference between this complex and the other complexes. From the figure, we found more NPA charges on nickels of the complexes bearing more electron-deficient ligands, which is in line with the tendency demonstrated in Figure 1. Moreover, electron-withdrawing groups, such as CF$_3$ and NO$_2$, seem to show more influence on the NPA charges of the nickel centers. Too great an NPA charge on the nickel center of our target complex **3h** may be the major reason for the instability of the complex, which makes it difficult to synthesize.

The synthesis of phosphine Ni^{II}−Ph complexes **4a**,**c**,**d** is shown in Scheme 4. The deprotonation of free ligands **2a**,**c**,**d** readily proceeded with excess sodium hydride in anhydrous THF for 4 h at room temperature, and the isolated sodium salts then reacted with an equivalent amount of *trans*-PhNi(PPh$_3$)$_2$Cl for 12 h in toluene to afford the neutral nickel complexes **4a**,**c**,**d**, respectively. The synthesis of complex **4b** has been reported in our previous publication.[20b]

Neutral nickel complexes **3a**−**g** and **4a**−**d** bearing β-ketiminato ligands have been clearly characterized by ^{1}H and ^{13}C NMR spectra as well as elemental analysis. To further confirm the structures of these complexes, single crystals of **3b**−**d**,**f**,**g** and **4a**,**c** suitable for X-ray crystallographic analysis were grown from a toluene−hexane solution. The data collection and refinement data of the analysis are summarized in Table 1, and the ORTEP diagrams are shown in Figures 3−7. In the solid state, these complexes adopt a nearly square planar coordination geometry, and the pyridine group or the phosphine group is trans to the N-aryl group, just as for the neutral nickel complexes reported previously.[20c,d]

The selected bond distances and angles are summarized in Table 2. For complexes **3b**−**d**, variation of the R group from the small phenyl through 1-naphthyl to the bulky 9-anthryl exhibits an obvious influence on the molecular structure obtained (see Figures 3 and 4). It is noteworthy that complex **3d** exhibits a shorter Ni−C(1) and a longer Ni−O bond distance in comparison to those of complexes **3b**,**c**, though they display similar Ni−N bond distances. There are no significant differences in O−C(8), N−C(10), and C(8)−C(9) bond distances for the three complexes, except that the C(9)−C(10) length for complex **3d** is much longer than those of complexes **3b**,**c** (see Table 2). Analogously, the angles around the nickel center of the three complexes are almost the same (see Table 2). However, the intriguing differences concerning the N(1)−Ni−N(2) and O−Ni−C(1) angles should not be ignored. As shown in Table 2, complex **3b** exhibits larger angles relative to complexes **3c**,**d**, indicating that **3b** has the least distortion in the nickel(II) coordination plane (see Figure 4). In contrast, such distortion is enhanced with regard to complexes **3c**,**d** due to the increased steric hindrance of the R group. The molecular structures of complexes **3b**−**d** from a view perpendicular to the nickel coordination plane are shown in Figure 4, indicating a great steric effect of the R group definitely confirmed by the increasing torsion angle O−C(8)−C(7)−C(6) for complexes **3b**−**d** from 2.83° through 35.77° to 69.36°.

Complexes **3f**,**g** were also synthesized to investigate the electronic effects of the substituted electron-donating or electron-withdrawing groups at the para positions. The electronic effects have showed a remarkable influence on the bond distances or angles of the complexes. Complex **3g** with a CF$_3$ group has Ni−O, Ni−C(1), and C(8)−C(9) bonds much shorter than those of the mother complex **3b** (see Table 2). More interestingly, both complexes **3f** (OMe) (see Figure 5) and **3g** (CF$_3$) exhibit larger O−C(8)−C(7)−C(6) torsion angles (19.33 and 13.19°) relative to complex **3b** (2.83°). In addition, in contrast to an electron-withdrawing group such as CF$_3$, an electron-donating group such as OMe would enlarge the O−C(8)−C(9)−C(10) torsion angle and decrease the C(8)−C(9)−C(10)−N(1) torsion angle, which may be caused by the influence of electron density on the nickel chelate ring.

dx.doi.org/10.1021/om2010194 | *Organometallics* 2012, 31, 966−975

Table 1. Crystal Data and Structure Refinement Details for Complexes 3b−d,f,g and 4a,c

	3b	3c	3d	3f	3g	4a	4c
empirical formula	$C_{27}H_{32}N_2NiO$	$C_{31}H_{34}N_2NiO$	$C_{42}H_{43}N_2NiO$	$C_{28}H_{34}N_2NiO_2$	$C_{28}H_{31}F_3N_2NiO$	$C_{43}H_{48}NNiOP$	$C_{49}H_{46}NNiOP$
formula wt	459.26	509.31	651.50	489.28	527.26	684.50	754.55
temp (K)	185(2)	185(2)	185(2)	185(2)	185(2)	185(2)	185(2)
cryst syst	monoclinic	triclinic	triclinic	monoclinic	monoclinic	monoclinic	monoclinic
space group	$P2_1/c$	$P\bar{1}$	$P\bar{1}$	$C2/c$	$C2/c$	$P2_1/n$	$P2_1/c$
a (Å)	12.6963(10)	9.7228(6)	10.8870(6)	20.7171(17)	20.8591(17)	10.4168(7)	13.5194(5)
b (Å)	20.8476(16)	9.7228(6)	13.3072(8)	14.5516(12)	15.3042(12)	24.7978(18)	11.3647(4)
c (Å)	9.6062(8)	13.013(8)	13.5337(8)	17.5100(15)	34.431(3)	14.4080(10)	25.5163(9)
α (deg)	90.00	60.7090(10)	70.6830(10)	90.00	90.00	90.00	90.00
β (deg)	106.66(10)	85.7880(10)	74.1560(10)	97.5690(10)	102.402(2)	96.6200(10)	89.9240(10)
γ (deg)	90.00	69.6070(10)	71.1360(10)	90.00	90.00	90.00	90.00
Z	4	2	2	8	16	4	4
V (Å^3)	2435.9(3)	1320.62(14)	1720.40(17)	5232.7(8)	10735.0(15)	3697.0(4)	3920.4(2)
ρ_{calcd} (Mg m^{-3})	1.252	1.281	1.258	1.242	1.305	1.230	1.278
abs coeff, (mm^{-1})	0.816	0.760	0.599	0.767	0.766	0.601	0.574
F(000)	976	540	692	2080	4416	1456	1592
θ range (deg)	1.67−26.03	1.81−26.02	1.62−26.04	1.72−26.05	1.66−25.05	1.64−25.70	1.51−26.05
no. of measd/indep rflns	14 519/4796	7219/5059	9418/6626	16 479/5170	31 220/9493	20 076/7017	21 308/7727
R_{int}	0.0379	0.0116	0.0130	0.0283	0.0710	0.0603	0.0212
abs cor	multiscan	multiscan	multiscan	multiscan	multiscan	multiscan	multiscan
max, min transmissn	0.929, 0.838	0.9347, 0.7875	0.953, 0.917	0.933, 0.863	0.8496, 0.7862	0.9535, 0.7993	0.950, 0.908
no. of params	280	316	415	298	641	431	482
final R indices ($I > 2\sigma(I)$)							
R1	0.0425	0.0342	0.0402	0.0405	0.0620	0.0491	0.0321
wR2	0.1010	0.0884	0.1070	0.1033	0.1301	0.0925	0.0837
goodness of fit on F^2	1.009	1.032	1.030	1.034	1.018	0.968	1.035
largest diff peak, hole (e Å^{-3})	0.459, −0.374	0.372, −0.353	0.543, −0.421	0.342, −0.357	0.627, −0.353	0.459, −0.236	0.543, −0.241

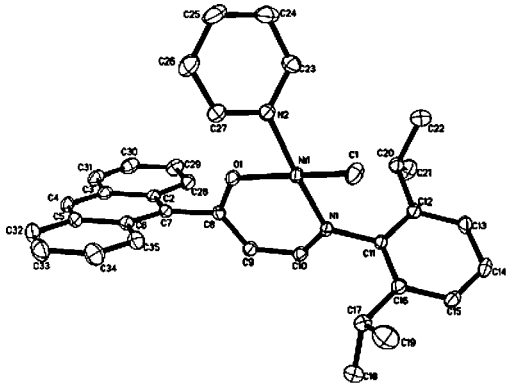

Figure 3. Molecular structure of complex **3d**. Thermal ellipsoids are drawn at the 30% probability level, and H atoms as well as a toluene molecule are omitted for clarity.

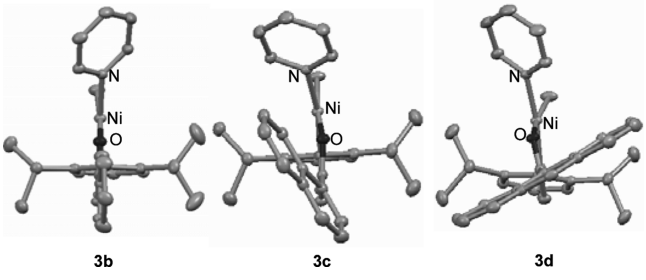

Figure 4. Molecular structures of complexes **3b−d.** Views are perpendicular to the nickel coordination plane.

The molecular structures of phosphine Ni^{II}−Ph complexes **4a,c** are shown in Figures 6 and 7. They display very different

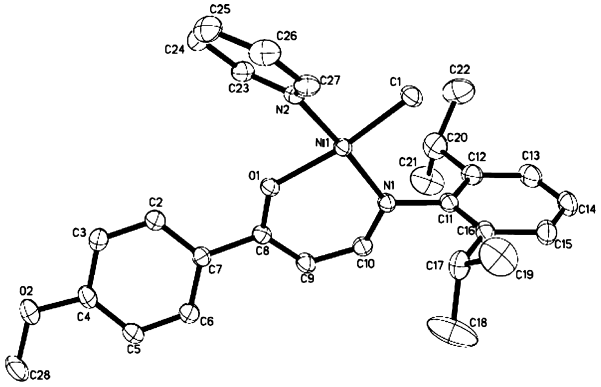

Figure 5. Molecular structure of complex **3f**. Thermal ellipsoids are drawn at the 30% probability level, and H atoms are omitted for clarity.

bond distances and angles as well as torsion angles in comparison with the pyridine Ni^{II}−Me complexes, probably due to the influence of the ancillary ligands (PPh_3 vs Py). As shown in Table 2, complex **4c** exhibits bond distances around the nickel centers very different from those of its analogue **3c** bearing the same ligand. Complex **4c** exhibits a Ni−O bond distance shorter than that of complex **3c**, and such a difference is more remarkable for the distance of Ni−C(1) indicating the large difference between a methyl group and a phenyl group connected to a nickel(II). In contrast, the Ni−N(1) bond length of complex **4c** is much longer that of complex **3c** (see Table 2) due to the distortion of the nickel chelate ring caused by the bulky PPh_3 group. In addition, the Ni−P bond (complex **4c**) is much longer than the Ni−N(2) bond (complex **3c**), which would have a great effect on the polymerization behavior.

dx.doi.org/10.1021/om2010194 | *Organometallics* 2012, 31, 966−975

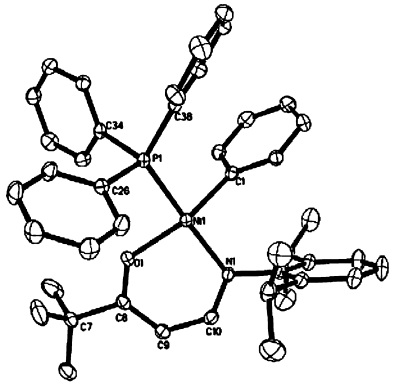

Figure 6. Molecular structure of complex **4a**. Thermal ellipsoids are drawn at the 30% probability level, and H atoms are omitted for clarity.

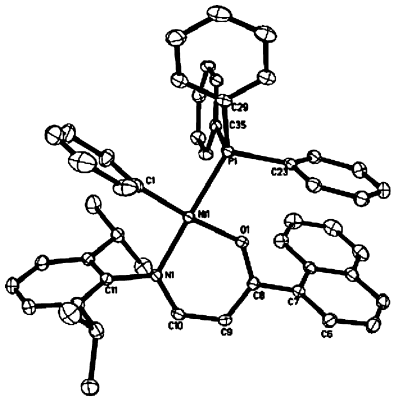

Figure 7. Molecular structure of complex **4c**. Thermal ellipsoids are drawn at the 30% probability level, and H atoms are omitted for clarity.

Complex **4c** exhibits larger angles of N(1)−Ni−P and O−Ni−C(1) relative to the corresponding angles of complex **3c**, indicating that **4c** has less distortion in the nickel(II) coordination plane (see Figure 7). Moreover, there are visible differences in the angles around the nickel centers of complexes **4c** and **3c**. As can be seen from Table 2, a much broader O−Ni−P angle of complex **4c** is observed relative to the O−Ni−N(2) angle of **3c**, compensated by the narrower angles of O−Ni−N(1), C(1)−Ni−N(1), and C(1)−Ni−P because of the steric congestion between the PPh_3 and R groups. The influence of the ancillary ligands (Py vs PPh_3) can also be confirmed by the much different torsion angles between complexes **4c** and **3c**. A much larger O−C(8)−C(7)−C(6) torsion angle (50.33°) for complex **4c** relative to complex **3c** (35.77°) is observed due to steric hindrance from the PPh_3 group. More interestingly, complex **4c** exhibits much larger torsion angles of O−C(8)−C(7)−C(6) and C(8)−C(9)−C(10)−N(1) (10.73 and 10.25°) relative to complex **3c** (0.58 and 3.05°). In a word, all the differences between the phosphine Ni^{II}−Ph complex and the pyridine Ni^{II}−Me complex may greatly influence the olefin polymerization behaviors.

Ethylene Polymerization with Pyridine Ni^{II}−Me Complexes 3a−g. Neutral nickel complexes **3a−g** were investigated as catalysts for ethylene polymerization in toluene. Typical results are summarized in Table 3. The data indicate that ligand structure can greatly affect the catalytic activity and polymer microstructure along with the properties. Complexes **3a−d** were synthesized to explore the steric effects of R groups on catalytic properties. Without a cocatalyst, catalyst **3a** (R = ^{t}Bu) showed a moderate activity of 36 (kg of PE)/((mol of Ni) h atm) (entry 3-1) under the typical conditions (70 °C, ethylene pressure 30 atm). In comparison, catalyst **3d** (R = 9-anthryl) exhibited a similar activity of 38 (kg of PE)/((mol of Ni) h atm) (entry 3-7) under the same conditions. However, lower activities (29 and 26 (kg of PE)/((mol of Ni) h atm), entries 3-3 and 3-5) of catalysts **3b,c** were observed because of their less bulky substituents relative to the 9-anthryl group. This is consistent with the notion that the neutral nickel salicylaldiminato catalyst also needs a bulky 9-anthryl group at the ortho position of the phenoxy group to achieve a high catalytic activity.[11] Herein, steric hindrance must have played an important role in stabilizing the active centers and enhancing

Table 2. Selected Bond Distances (Å) and Angles (deg)

	3b	3c	3d	3f	3g	4a	4c
			Bond Distances				
Ni−O	1.916(18)	1.912(13)	1.922(13)	1.918(15)	1.897(3)	1.912(17)	1.897(11)
Ni−N(1)	1.893(2)	1.880(15)	1.894(15)	1.894(18)	1.889(3)	1.915(2)	1.929(13)
Ni−(N(2) or P)	1.914(2)	1.912(15)	1.911(16)	1.919(18)	1.916(3)	2.176(8)	2.202(4)
Ni−C(1)	1.929(3)	1.924(2)	1.913(2)	1.924(2)	1.911(4)	1.884(3)	1.886(17)
O−C(8)	1.275(3)	1.277(2)	1.280(2)	1.280(3)	1.283(5)	1.283(3)	1.282(19)
N(1)−C(10)	1.314(3)	1.326(2)	1.316(2)	1.317(3)	1.317(5)	1.306(3)	1.318(2)
C(8)−C(9)	1.386(4)	1.394(3)	1.377(3)	1.384(3)	1.371(5)	1.376(4)	1.386(2)
C(9)−C(10)	1.393(4)	1.390(3)	1.413(3)	1.398(3)	1.396(6)	1.403(4)	1.399(2)
			Bond Angles				
N(1)−Ni−(N(2) or P)	176.00(8)	170.92(7)	172.95(7)	172.93(8)	172.80(15)	163.23(7)	175.71(4)
O−Ni−C(1)	172.12(10)	170.37(8)	166.29(9)	172.15(9)	172.53(16)	158.84(10)	174.45(6)
O−Ni−N(1)	93.72(8)	93.89(6)	94.61(6)	93.37(7)	93.22(13)	93.93(9)	91.56(5)
O−Ni−-(N(2) or P)	84.23(8)	83.31(6)	84.39(6)	84.22(7)	83.72(13)	88.59(6)	85.55(4)
C(1)−Ni−N(1)	93.20(11)	94.07(8)	93.76(8)	93.08(9)	93.32(16)	95.33(11)	93.90(6)
C(1)−Ni−(N(2) or P)	89.08(11)	89.62(8)	88.60(8)	89.88(9)	90.22(16)	88.00(9)	88.95(5)
			Torsion Angles				
O−C(8)−C(7)−C(6)	2.83	35.77	69.36	19.33	13.19		50.33
O−C(8)−C(9)−C(10)	2.38	0.58	1.47	4.26	0.31	0.71	10.73
C(8)−C(9)−C(10)−N(1)	2.96	3.05	6.75	0.12	3.08	7.65	10.25

dx.doi.org/10.1021/om2010194 | *Organometallics* 2012, 31, 966−975

Table 3. Results of Ethylene Polymerization Reactions for Complexes 3a−g[a]

entry	complex (amt (μmol))	T (°C)	pressure (atm)	amt of polymer (g)	activity[b]	T_m (°C)	M_w[c] (kg/mol)	.	branches[d]/1000C
3-1	**3a** (20)	70	30	7.2	36	106	26.2	1.8	27
3-2[e]	**3a** (20)	60	20	2.5	19	105	24.9	1.8	nd
3-3	**3b** (20)	70	30	5.7	29	99	25.2	1.9	32
3-4	**3c** (20)	60	30	1.1	5.5	101	28.5	2.0	37
3-5	**3c** (20)	70	30	5.1	26	94	21.9	1.9	46
3-6	**3c** (20)	80	30	1.5	7.5	82	10.8	2.0	66
3-7	**3d** (20)	70	30	7.5	38	94	18.6	1.9	49
3-8[e]	**3d** (20)	70	20	14	105	94	20.9	1.9	nd
3-9[e]	**3e** (20)	70	20	1.1	8.3	106	33.2	2.0	35
3-10	**3f** (20)	70	20	5.3	40	87	18.5	1.8	nd
3-11[e]	**3f** (10)	70	20	2.2	33	103	31.9	1.8	37
3-12[e]	**3g** (20)	70−77	20	12.8	96	96	22.8	1.8	40

[a]Reaction conditions: 100 mL of toluene, polymerization for 20 min. [b]In units of (kg of PE)/((mol of Ni) h atm). [c]Determined by GPC. [d]Calculated from ^{1}H NMR. [e]Two equivalents of $B(C_6F_5)_3$ added.

the catalytic activities of the neutral nickel β-ketiminato catalysts. In addition, catalyst **3d** exhibited a high activity of up to 105 (kg of PE)/((mol of Ni) h atm) (entry 8) upon the addition of $B(C_6F_5)_3$.

The steric hindrance can also greatly affect the molecular weight (MW) as well as the branching content of the polymers obtained. As shown in Table 3, with regard to catalysts **3b−d**, the weight-average molecular weight (M_w) decreases from 25.2 through 21.9 to 18.6 kg/mol (entries 3-3, 3-5, and 3-7), with the steric hindrance increasing from a phenyl through a 1-naphthyl to a 9-anthryl group. Nevertheless, an enhancement of the branching content from 32 to 49 branches per 1000 carbon atoms (entries 3-3, 3-5, and 3-7) was observed. As we know, there is a competitive relationship between the ethylene insertion reaction and the chain transfer reaction, which determines the molecular weight of the polyethylene produced. For the neutral nickel β-ketiminato catalysts, bulky ligands would not only suppress the chain transfer reaction but also decrease the ethylene insertion rate according to the DFT results in our previous report.[20d] The decreased MW can be best explained by the reduced value of (chain propagation rate)/(chain walking rate) due to the steric effects.

As shown in Table 3, complex **3e** with a strongly electron-donating NMe_2 group in the para position showed a much lower activity of 8.3 (kg of PE)/((mol of Ni) h atm) (entry 3-9) relative to that of mother catalyst **3b** (29 (kg of PE)/((mol of Ni) h atm)), although $B(C_6F_5)_3$ was added as the cocatalyst. In contrast, a higher activity of 40 (kg of PE)/((mol of Ni) h atm) (entry 3-10) was observed using catalyst **3f** with an OMe group. Therefore, we can not simply ascribe the greatly decreased activity of **3e** to the electronic effect of the NMe_2 group; the possibly direct interaction between NMe_2 groups and nickel(II) centers may be partly responsible for the issue. In addition, complex **3g** with a *p*-CF_3 showed an activity of 96 (kg of PE)/((mol of Ni) h atm) (entry 3-12), higher than that for the mother complex **3b**.

The electronic factors can also greatly influence the MW as well as the branching content of the polyethylene obtained. It can be generally observed from the data (Table 3) that polymers with higher MWs have been produced by catalysts bearing more electron-donating ligands. The MW of the polymer produced by **3e** with an NMe_2 group is higher than that of catalyst **3g** with a CF_3 group (entry 3-9 vs 3-12). In contrast, catalysts with more electron deficient ligands prefer to produce the polyethylene with more branching content, which can be attributed to the accelerated chain-walking reaction caused by the electronic perturbation of the nickel(II) centers. A similar effect of the electron-withdrawing substituents strongly enhancing chain termination over chain propagation was also found in ethylene oligomerization with the SHOP catalyst.[23]

Reaction conditions, such as reaction temperature and ethylene pressure, also dramatically influence the catalytic activity as well as the MW and branching number. For **3c**, the catalytic activity was greatly enhanced from 5.5 to 26 (kg of PE)/((mol of Ni) h atm) via increasing the reaction temperature from 60 to 70 °C (entries 3-4 and 3-5). However, further elevating the temperature to 80 °C caused a lower catalytic activity of 7.5 (kg of PE)/((mol of Ni) h atm) (entry 3-6). The lower equilibrium concentration of ethylene in solution as well as the catalyst instability at 80 °C relative to 70 °C may be mainly responsible for the difference. As shown in Table 3, the amount of polymer produced by catalysts **3a** is greatly influenced by ethylene pressure. A much lower productivity (entries 3-1 and 3-2) was observed by decreasing the ethylene pressure from 30 to 20 atm. Additionally, the MWs of the polyethylenes produced by catalyst **3c** decreased from 28.5 to 10.8 kg/mol by increasing the reaction temperature from 60 to 80 °C, and the branch contents were enhanced from 37 to 66 branches per 1000 carbon atoms (entries 3-4−3-6). A similar phenomenon has also been reported concerning α-diimine cationic nickel catalysts as well as the neutral nickel salicylaldiminato systems,[1a,11] demonstrating that the rate of chain migration and termination in our systems also increased at elevated temperature, yielding more highly branched and lower MW polymer.

The microstructure of the typical polyethylene obtained has been definitely characterized using ^{1}H and ^{13}C NMR, as shown in Figure 8. In Figure 8a (^{1}H NMR), the signal at about 0.8 ppm can be assigned to methyl branches that are the predominant branching style in the polymers produced under 30 atm (entry 3-1).[24a] Moreover, as shown in Figure 8b (^{13}C NMR), methyl branches are the only type of branches in the polymer chain produced by **3a** (entry 3-1).[24b] The melting points of polymers decrease with an increase of branching number (Table 3), because branches can restrain the crystallization of the polymers. The low PDI (M_w/M_n = 1.8−2.0) of the obtained polyethylene indicates that these neutral nickel complexes are favorable homogeneous single-site catalysts.

dx.doi.org/10.1021/om2010194 | Organometallics 2012, 31, 966−975

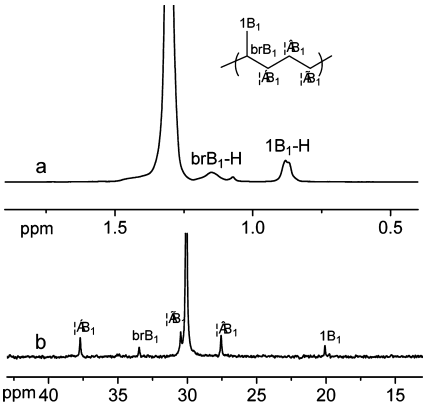

Figure 8. (a) ^{1}H and (b) ^{13}C NMR spectra of polyethylene produced by **3a** (entry 1), assigned according to the literature.[24]

Ethylene Polymerization with Phosphine Ni^{II}–Ph Complexes 4a–d. Phosphine Ni^{II}–Ph complexes **4a–d** were also investigated as catalysts for ethylene polymerization to find out their differences from pyridine Ni^{II}–Me complexes **3a–d** in catalytic performance. The typical polymerization data in Table 4 indicate that the variation of the R group can also be effective for the modulation of catalytic properties. At a reaction temperature of 60 °C, catalyst **4a** (R = ^{t}Bu) showed a moderate activity of 42 (kg of PE)/((mol of Ni) h atm) (entry 4-1), which is much higher than that of catalyst **3a** (19 (kg of PE)/((mol of Ni) h atm), entry 3-2, Table 3). In the absence of a cocatalyst, complex **4d** (R = 9-anthryl) showed an activity (105 (kg of PE)/((mol of Ni) h atm), entry 4-7) higher than those of complexes **4b,c** (75 and 65 (kg of PE)/((mol of Ni) h atm), entries 4-2 and 4-4) under the typical polymerization conditions (60 °C, 20 atm). In comparison with **4d**, the pyridine Ni^{II}–Me complex **3d** exhibited the same activity but in the presence of $B(C_6F_5)_3$ at a higher reaction temperature of 70 °C. A possible reason is that the dissociation of PPh_3 from the nickel center seems to be easier than that of a pyridine because of more steric congestion of the bulky PPh_3 with the R group (see the single-crystal structure). As shown in Table 4, the variation of the ligand structure is an efficient methodology to control the molecular weight (MW) of the polyethylene obtained. Polyethylenes with different MWs ranging from 28.4 to 15.0 kg/mol (see entries 4-1, 4-2, 4-4, and 4-7) were prepared under the same reaction conditions using catalysts **4a–d** bearing different ligands. Different R groups with variable steric effects should be the determining factor for the MW of polyethylene, which has also been supported by the polymerization results for catalysts **3b–d** (see Table 3).

Table 4. Results of Ethylene Polymerization Reactions for Complexes 4a–d[a]

entry	complex	T (°C)	amt of polymer (g)	activity[b]	T_m (°C)	M_w[c] (kg/mol)	M_w/M_n[c]
4-1[d]	**4a**	60	9.7	42	105	28.4	1.9
4-2	**4b**	60	10	75	103	26.9	1.8
4-3	**4c**	50	1.9	14	99	27.3	1.9
4-4	**4c**	60	8.6	65	88	18.2	2.0
4-5	**4c**	70	6.0	45	82	10.6	1.9
4-6[d]	**4c**	60	11	47	101	30.8	2.0
4-7	**4d**	60	14	105	86	15.0	1.9
4-8[d]	**4d**	60	15	64	95	17.9	2.2

[a]Reaction conditions: 100 mL of toluene, 20 μmol of catalyst, ethylene pressure of 20 atm, polymerization for 20 min. [b]In units of (kg of PE)/((mol of Ni) h atm). [c]Determined by GPC. [d]The ethylene pressure is 35 atm.

Similar to the case for catalysts **3b–d**, the reaction temperature can greatly influence the catalytic properties of catalysts **4a–d**. For **4c**, a great increase of the activity from 14 to 65 (kg of PE)/((mol of Ni) h atm) (entries 4-3 and 4-4) was observed by elevating the reaction temperature from 50 to 60 °C, but higher temperature (70 °C) leads to a decrease of the activity. This is different from the case for catalyst **3c**, which showed the highest activity at 70 °C, suggesting that the pyridine complexes need more energy than the phosphine complexes to be efficiently activated for the ethylene polymerization in our systems. In addition, polyethylenes with lower molecular weights (MWs) were produced by catalyst **4c** upon increasing the reaction temperature because of the accelerated chain-walking reaction, which is the same as that for the pyridine catalyst **3c**.

CONCLUSIONS

We have proved that a family of newly designed neutral nickel complexes **3a–g** and **4a–d** based on various β-ketiminato ligands is highly active for ethylene polymerization. Ligand steric and electronic effects have been confirmed to greatly influence the catalytic behavior. Complexes with more bulky ligands were found to be more active, producing polyethylene with lower molecular weight and higher branching number. Catalyst **3g**, with a strongly electron-withdrawing group (CF_3), showed an activity much higher than the value for the mother catalyst **3b**. In contrast, a much lower activity of catalyst **3e** was observed due to the strongly electron-donating group (NMe_2) on the ligand. Moreover, electron-deficient ligands were found to decrease the molecular weight and enhance the branching content of the polyethylene obtained. In addition, phosphine Ni^{II}–Ph complexes **4a–d** showed higher activities relative to pyridine Ni^{II}–Me complexes **3a–d** because of the different ancillary ligands (PPh_3 vs Py) on the nickel centers.

EXPERIMENTAL SECTION

General Procedures and Materials. All work involving air- and/or moisture-sensitive compounds was carried out under a dry nitrogen atmosphere by using standard Schlenk techniques or under a dry argon atmosphere in an MBraun glovebox unless otherwise noted. All solvents used were purified from an MBraun SPS system. The NMR data of ligands and complexes were obtained on a Bruker 300 MHz spectrometer at ambient temperature with $CDCl_3$ or C_6D_6 as the solvent. The NMR analyses of polymers were performed on a Varian Unity 400 MHz spectrometer at 135 °C, using *o*-$C_6D_4Cl_2$ as the solvent. The differential scanning calorimetric (DSC) measurements were performed with a PerkinElmer Pyris 1 DSC differential scanning calorimeter at a rate of 10 °C/min. The molecular weights and the polydispersities of the polymer samples were determined at 150 °C by a PL-GPC 220 type high-temperature chromatograph equipped with three PLgel 10 μm Mixed-B LS type columns. 1,2,4-Trichlorobenzene (TCB) was employed as the solvent at a flow rate of 1.0 mL/min. The calibration was made by polystyrene standard EasiCal PS-1 (PL Ltd.).

Pinacolone, 1-acetonaphthone, and 9-anthracenone were purchased from Aldrich Chemicals and directly used without purification. 2,6-Diisopropylaniline and NaH were obtained from Acros. Potassium *tert*-butoxide was purchased from Aldrich Chemicals. $Py_2Ni(CH_3)_2$ and *trans*-$PhNi(PPh_3)_2Cl$ were prepared according to the literature.[25] Commercial ethylene was used without further purification.

Synthesis of Ligands 2a–h. To a slurry of 3.3 g of potassium *tert*-butoxide (1.5 equiv) in anhydrous diethyl ether (40 mL) were added

dx.doi.org/10.1021/om2010194 | *Organometallics* 2012, 31, 966–975

2.0 g of pinacolone (20 mmol) and 2.9 g of ethyl formate (2.0 equiv) at 0 °C. Immediately a large amount of white solid appeared in the reaction bottle, and the mixture was stirred for 30 min at 0 °C. Then the resulting suspension was warmed to room temperature and stirred for about 10 h. The white solid was separated by filtration and dried under reduced pressure. Formic acid in ethanol was added to the solid until the pH <7, affording the corresponding β-diketone, which was used directly in the preparation of ligand **2a**. Subsequently, 3.5 g of 2,6-diisopropylaniline (1.0 equiv) was added to the obtained β-diketone in ethanol and the condensation reaction was carried out for about 24 h, yielding 3.3 g of ligand **2a** (58%). Ligands **2b**−**h** were prepared according to the same method as for **2a**.

(2,6-^{i}Pr$_2$C$_6$H$_3$)N═CHCHC(^{t}Bu)OH (**2a**). ^{1}H NMR (300 MHz, $CDCl_3$): δ 11.10 (d, $^3J_{HH}$ = 12.0 Hz, 1H, N−H), 7.25−7.14 (m, 3H, Ar H), 6.69 (dd, $^3J_{HH}$ = 12.6, 7.8 Hz, 1H, N═C−H), 5.38 (d, $^3J_{HH}$ = 7.8 Hz, 1H, C═CH), 3.19 (sept, $^3J_{HH}$ = 6.9 Hz, 2H, ^{i}Pr CH), 1.22 (s, 9H, ^{t}Bu H), 1.20 (d, $^3J_{HH}$ = 6.9 Hz, 12H, ^{i}Pr CH_3). ^{13}C NMR (300 MHz, $CDCl_3$): δ 207.49 (N═C), 153.22, 144.93, 136.88, 127.66, 124.11, (Ar), 90.91 (═C), 28.61 (^{i}Pr CH), 28.08 (^{t}Bu), 24.21 (^{i}Pr CH_3). Anal. Calcd for $C_{19}H_{29}NO$: C, 79.39; H, 10.17; N, 4.87. Found: C, 73.32; H, 10.12; N, 4.93.

(2,6-^{i}Pr$_2$C$_6$H$_3$)N═CHCHC(Ph)OH (**2b**). The synthesis of the ligand has been reported in our previous work.[20d]

(2,6-^{i}Pr$_2$C$_6$H$_3$)N═CHCHC(1-naphthyl)OH (**2c**). Yield: 65%. ^{1}H NMR (300 MHz, $CDCl_3$): δ 11.73 (d, J = 12.0 Hz, 1H, N−H), 8.58 (d, $^3J_{HH}$ = 8.1 Hz, 1H, Ar H), 7.93−7.77 (m, 3H, Ar H), 7.60−7.47 (m, 3H, Ar H), 7.32−7.20 (m, 3H, Ar H), 6.94 (dd, $^3J_{HH}$ = 12.6, 7.5 Hz, 1H, N═CH), 5.75 (d, $^3J_{HH}$ = 7.5 Hz, 1H, C═CH), 3.33 (sept, $^3J_{HH}$ = 6.9 Hz, 2H, ^{i}Pr CH), 1.28 (d, $^3J_{HH}$ = 6.9 Hz, 12H, ^{i}Pr CH_3). ^{13}C NMR (300 MHz, $CDCl_3$): δ 195.42 (N═C), 154.17, 144.95, 139.68, 136.63, 134.31, 130.82, 128.70, 127.15, 126.51, 126.42, 126.38, 125.20, 124.28, (Ar), 96.71 (═C), 28.85 (^{i}Pr CH), 24.27 (^{i}Pr CH_3). Anal. Calcd for $C_{25}H_{27}NO$: C, 83.99; H, 7.61; N, 3.92. Found: C, 83.87; H, 7.66; N, 3.97.

(2,6-^{i}Pr$_2$C$_6$H$_3$)N═CHCHC(9-anthryl)OH (**2d**). Yield: 62%. ^{1}H NMR (300 MHz, $CDCl_3$): δ 11.94 (d, J = 12.3 Hz, 1H, N−H), 8.47 (s, 1H, Ar H), 8.23−8.01 (m, 4H, Ar H), 7.53−7.24 (m, 7H, Ar H), 6.97 (dd, $^3J_{HH}$ = 12.6, 7.2 Hz, 1H, N═CH), 5.67 (d, $^3J_{HH}$ = 7.2 Hz, 1H, C═CH), 3.43 (sept, $^3J_{HH}$ = 6.6 Hz, 2H, ^{i}Pr CH), 1.35 (d, $^3J_{HH}$ = 6.9 Hz, 12H, ^{i}Pr CH_3). ^{13}C NMR (300 MHz, $CDCl_3$): δ 196.94 (N═C), 153.82, 144.84, 137.84, 136.53, 131.67, 128.88, 128.23, 128.10, 127.90, 126.39, 126.20, 125.69, 124.35, (Ar), 99.72 (═C), 28.98 (^{i}Pr CH), 24.25 (^{i}Pr CH_3). Anal. Calcd for $C_{29}H_{29}NO$: C, 85.47; H, 7.17; N, 3.44. Found: C, 85.39; H, 7.13; N, 3.39.

(2,6-^{i}Pr$_2$C$_6$H$_3$)N═CHCHC(p-Me$_2$NPh)OH (**2e**). Yield: 55%. ^{1}H NMR (300 MHz, $CDCl_3$): δ 11.51 (d, J = 12.0 Hz, 1H, N−H), 7.92 (d, $^3J_{HH}$ = 6.0 Hz, 2H, Ar H), 7.26−7.17 (m, 3H, Ar H), 6.83 (dd, $^3J_{HH}$ = 12.3, 7.8 Hz, 1H, N═CH), 6.71 (d, $^3J_{HH}$ = 9.0 Hz, 2H, Ar H), 5.91 (d, $^3J_{HH}$ = 7.8 Hz, 1H, C═CH), 3.29 (sept, $^3J_{HH}$ = 6.9 Hz, 2H, ^{i}Pr CH), 3.06 (s, 3H, NCH_3), 1.22 (d, $^3J_{HH}$ = 6.9 Hz, 12H, ^{i}Pr CH_3). ^{13}C NMR (300 MHz, $CDCl_3$): δ 190.34 (N═C), 152.92, 145.05, 137.11, 129.56, 127.65, 124.14, 111.40, (Ar), 91.49 (═C), 40.55 (NMe), 28.71 (^{i}Pr CH), 24.28 (^{i}Pr CH_3). Anal. Calcd for $C_{23}H_{30}N_2O$: C, 78.82; H, 8.63; N, 7.99. Found: C, 78.92; H, 8.57; N, 7.96.

(2,6-^{i}Pr$_2$C$_6$H$_3$)N═CHCHC(p-MeOPh)OH (**2f**). Yield: 60%. ^{1}H NMR (300 MHz, $CDCl_3$): δ 11.58 (d, J = 12.3 Hz, 1H, N−H), 7.96 (m, 2H, Ar H), 7.30−7.18 (m, 3H, Ar H), 6.97−6.86 (m, 3H, Ar H), 5.92 (d, $^3J_{HH}$ = 7.5 Hz, 1H, C═CH), 3.88 (s, 3H, OCH_3), 3.26 (sept, $^3J_{HH}$ = 6.9 Hz, 2H, ^{i}Pr CH), 1.23 (d, $^3J_{HH}$ = 6.9 Hz, 12H, ^{i}Pr CH_3). ^{13}C NMR (300 MHz, $CDCl_3$): δ 190.22 (N═C), 162.64, 153.92, 145.04, 136.78, 132.57, 129.67, 127.93, 124.19, 113.97 (Ar), 91.53 (═C), 55.75 (OMe), 28.75 (^{i}Pr CH), 24.24 (^{i}Pr CH_3). Anal. Calcd for $C_{22}H_{27}NO_2$: C, 78.30; H, 8.06; N, 4.15. Found: C, 78.38; H, 8.02; N, 4.12.

(2,6-^{i}Pr$_2$C$_6$H$_3$)N═CHCHC(p-F$_3$CPh)OH (**2g**). Yield: 63%. ^{1}H NMR (300 MHz, $CDCl_3$): δ 11.75 (d, J = 12.3 Hz, 1H, N−H), 8.06 (m, 2H, Ar H), 7.72 (m, 2H, Ar H), 7.72 (m, 3H, Ar H), 7.0 (m, 3H, Ar H), 5.95 (m, 1H, C═CH), 3.22 (sept, $^3J_{HH}$ = 6.9 Hz, 2H, ^{i}Pr CH), 1.24 (d, $^3J_{HH}$ = 6.9 Hz, 12H, ^{i}Pr CH_3). ^{13}C NMR (300 MHz, $CDCl_3$): δ 189.40 (N═C), 155.33, 144.96, 142.88, 136.29, 128.31, 127.97, 125.74, 124.26, (Ar), 91.85 (═C), 28.79 (^{i}Pr CH), 24.17 (^{i}Pr CH_3). Anal. Calcd for $C_{22}H_{24}F_3NO$: C, 70.38; H, 6.44; N, 3.73. Found: C, 70.45; H, 6.38; N, 3.78.

(2,6-^{i}Pr$_2$C$_6$H$_3$)N═CHCHC(p-O$_2$NPh)OH (**2h**). Yield: 21%. ^{1}H NMR (300 MHz, $CDCl_3$): δ 11.82 (d, J = 12.6 Hz, 1H, N−H), 8.31 (d, J = 8.7 Hz, 2H, Ar H), 8.11 (d, J = 8.7 Hz, 2H, Ar H), 7.34−7.21 (m, 3H, Ar H), 7.04 (dd, J = 12.6, 7.2 Hz, 1H, N═CH), 5.96 (d, J = 7.2 Hz, 1H, C═CH), 3.21 (sept, ^3J = 6.9 Hz, 2H, ^{i}Pr CH), 1.24 (d, ^3J = 6.9 Hz, 12H, ^{i}Pr CH_3). ^{13}C NMR (300 MHz, $CDCl_3$): δ 187.90 (N═C), 155.46, 149.26, 144.78, 144.53, 135.69, 128.21, 128.11, 123.93, 126.63 (Ar), 91.69 (═C), 28.44 (^{i}Pr CH), 23.79 (^{i}Pr CH_3). Anal. Calcd for $C_{21}H_{24}N_2O_3$: C, 71.57; H, 6.86; N, 7.95. Found: C, 71.51; H, 6.81; N, 7.90.

Synthesis of Complexes 3a−g. To (pyridine)$_2$NiMe$_2$ (0.27 g, 1.1 mmol) and the ligand **2a** (0.29 g, 1.0 mmol) in a 100 mL septum-capped Schlenk bottle was added toluene (15 mL) at 25 °C. Immediate methane evolution was observed, which ceased within 5−10 min. The resulting red solution was stirred for an additional 4 h at 25 °C, during which time excess (pyridine)$_2$NiMe$_2$ decomposed to nickel black. The resulting mixture was filtrated to remove nickel black, the residue was extracted with toluene, and all volatiles were removed under reduced pressure to yield pure samples of pyridine complex **3a** as a red powder in high yield (89%). The other neutral nickel(II) complexes **3b**−**g** were prepared by the same procedure with similar yields.

[(2,6-^{i}Pr$_2$C$_6$H$_3$)N═CHCHC(^{t}Bu)O]Ni(Py)(CH$_3$) (**3a**). ^{1}H NMR (300 MHz, C_6D_6): δ 8.68 (d, $^3J_{HH}$ = 5.1 Hz, 2H, *o*-H Py), 7.09−6.89 (m, 3H, Ar H), 6.61 (t, $^3J_{HH}$ = 7.8 Hz, 1H, *p*-H Py), 6.22 (t, $^3J_{HH}$ = 6.9 Hz, *m*-H Py), 5.31 (d, $^3J_{HH}$ = 6.3 Hz, 1H, C═CH), 4.36 (sept, $^3J_{HH}$ = 6.9 Hz, 2H, ^{i}Pr CH), 1.53, 1.23, (d, $^3J_{HH}$ = 6.9 Hz, 12H, ^{i}Pr CH_3), 1.11 (s, 9H, ^{t}Bu H), −0.60 (s, 3H, $NiCH_3$). ^{13}C NMR (600 MHz, C_6D_6): δ 187.97 (NC), 151.69, 142.28, 135.28, 125.48, 123.14, 122.66, (Ar, Py), 89.73 (═C), 38.88 (^{t}Bu C), 28.41 (^{t}Bu CH_3), 28.03 (^{i}Pr CH), 24.91, 23.11, (^{i}Pr CH_3), −7.14 ($NiCH_3$). Anal. Calcd for $C_{25}H_{36}NNiO$: C, 68.36; H, 8.26; N, 6.38. Found: C, 68.30; H, 8.21; N, 6.39.

[(2,6-^{i}Pr$_2$C$_6$H$_3$)N═CHCHC(Ph)O]Ni(Py)(CH$_3$) (**3b**). The synthesis of the complex has been reported in our previous work.[20d]

[(2,6-^{i}Pr$_2$C$_6$H$_3$)N═CHCHC(1-naphthyl)O]Ni(Py)(CH$_3$) (**3c**). Yield: 91%. ^{1}H NMR (300 MHz, C_6D_6): δ 8.68 (d, $^3J_{HH}$ = 5.1 Hz, 2H, *o*-H Py), 7.09−6.89 (m, 3H, Ar H), 6.61 (t, $^3J_{HH}$ = 7.8 Hz, 1H, *p*-H Py), 6.22 (t, $^3J_{HH}$ = 6.9 Hz, *m*-H Py), 5.31 (d, $^3J_{HH}$ = 6.3 Hz, 1H, C═CH), 4.36 (sept, $^3J_{HH}$ = 6.9 Hz, 2H, ^{i}Pr CH), 1.53, 1.23, (d, $^3J_{HH}$ = 6.9 Hz, 12H, ^{i}Pr CH_3), 1.11 (s, 9H, ^{t}Bu H), −0.60 (s, 3H, $NiCH_3$). ^{13}C NMR (600 MHz, C_6D_6): δ 177.04 (NC), 160.13, 151.57, 150.91, 142.07, 139.85, 135.26, 134.20, 131.12, 128.90, 127.04, 125.70, 125.41, 124.96, 123.25, 122.88 (Ar, Py), 96.95 (═C), 28.24 (^{i}Pr CH), 24.93, 23.19 (^{i}Pr CH_3), −6.79 ($NiCH_3$). Anal. Calcd for $C_{31}H_{34}N_2NiO$: C, 73.11; H, 6.73; N, 5.50. Found: C, 73.18; H, 6.70; N, 5.54.

[(2,6-^{i}Pr$_2$C$_6$H$_3$)N═CHCHC(9-anthryl)O]Ni(Py)(CH$_3$) (**3d**). Yield: 93%. ^{1}H NMR (300 MHz, C_6D_6): δ 8.69 (d, $^3J_{HH}$ = 8.7 Hz, 2H, Ar H), 8.62 (d, $^3J_{HH}$ = 5.1 Hz, 2H, *o*-H Py), 8.05 (s, 1H, Ar H), 7.72 (d, $^3J_{HH}$ = 7.8 Hz, 2H, Ar H), 7.31−7.00 (m, 6H, Ar H), 6.25 (t, $^3J_{HH}$ = 7.8 Hz, 1H, *p*-H Py), 5.87 (t, $^3J_{HH}$ = 6.9 Hz, *m*-H Py), 5.56 (d, $^3J_{HH}$ = 6.0 Hz, 1H, C═C−H), 4.71 (sept, $^3J_{HH}$ = 6.9 Hz, 2H, ^{i}Pr CH), 1.66, 1.38 (d, $^3J_{HH}$ = 6.9 Hz, 12H, ^{i}Pr CH_3), −0.45 (s, 3H, $NiCH_3$). ^{13}C NMR (600 MHz, C_6D_6): δ 176.26 (NC), 159.71, 151.45, 150.97, 141.99, 138.36, 135.12, 131.63, 129.03, 128.64, 128.29, 128.04, 127.01, 126.73, 125.74, 125.36, 125.01, 123.31, 122.82 (Ar, Py), 100.04 (═C), 28.47 (^{i}Pr CH), 24.95, 23.23 (^{i}Pr CH_3), −6.49 ($NiCH_3$). Anal. Calcd for $C_{35}H_{36}N_2NiO$: C, 75.15; H, 6.49; N, 5.01. Found: C, 75.08; H, 6.51; N, 5.06.

[(2,6-^{i}Pr$_2$C$_6$H$_3$)N═CHCHC(p-Me$_2$NPh)O]Ni(Py)(CH$_3$) (**3e**). Yield: 89%. ^{1}H NMR (300 MHz, C_6D_6): δ 8.82 (d, $^3J_{HH}$ = 5.1 Hz, 2H, *o*-H Py), 7.88 (d, 2H, J = 8.7 Hz, Ar H), 7.29−7.15 (m, 3H, Ar H), 6.74 (t, $^3J_{HH}$ = 7.8 Hz, 1H, *p*-H Py), 6.52 (d, 2H, J = 8.7 Hz, Ar H), 6.37 (t, $^3J_{HH}$ = 6.9 Hz, *m*-H Py), 6.06 (d, $^3J_{HH}$ = 6.6 Hz, 1H, C═CH), 4.59 (sept, $^3J_{HH}$ = 6.9 Hz, 2H, ^{i}Pr CH), 2.49 (s, 6H, NCH_3), 1.71, 1.38, (d, $^3J_{HH}$ = 6.9 Hz, 12H, ^{i}Pr CH_3), −0.46 (s, 3H, $NiCH_3$). ^{13}C NMR (600 MHz, C_6D_6): δ 173.28 (NC), 159.48, 151.85, 151.40, 151.17, 142.47, 135.15, 125.43, 123.13, 122.74, 111.36 (Ar, Py), 90.74 (═C), 39.44

dx.doi.org/10.1021/om2010194 | *Organometallics* 2012, 31, 966−975

(NCH_3), 28.13 (^{i}Pr CH), 24.95, 23.23 (^{i}Pr CH_3), −6.97 ($NiCH_3$). Anal. Calcd for $C_{29}H_{37}N_3NiO$: C, 69.34; H, 7.42; N, 8.37. Found: C, 69.24; H, 7.45; N, 8.32.

[(2,6-^{i}Pr$_2$C$_6$H$_3$)N═CHCHC(p-MeOPh)O]Ni(Py)(CH$_3$) ***(3f)***. Yield: 87%. ^{1}H NMR (300 MHz, C_6D_6): δ 8.75 (d, $^3J_{HH}$ = 5.1 Hz, 2H, *o*-H Py), 7.79 (d, 2H, *J* = 8.4 Hz, Ar H), 7.26−7.13 (m, 3H, Ar H), 6.74 (d, 2H, *J* = 8.4 Hz, Ar H), 6.68 (t, $^3J_{HH}$ = 7.8 Hz, 1H, *p*-H Py), 6.30 (t, $^3J_{HH}$ = 6.9 Hz, *m*-H Py), 5.93 (d, $^3J_{HH}$ = 6.6 Hz, 1H, C═CH), 4.53 (sept, $^3J_{HH}$ = 6.9 Hz, 2H, ^{i}Pr CH), 3.26 (s, 3H, OCH_3), 1.68, 1.35, (d, $^3J_{HH}$ = 6.9 Hz, 12H, ^{i}Pr CH_3), −0.47 (s, 3H, $NiCH_3$). ^{13}C NMR (600 MHz, C_6D_6): δ 172.45 (NC), 160.92, 159.93, 151.72, 151.13, 142.24, 135.28, 132.40, 128.07, 125.58, 123.18, 122.81, 113.39, (Ar, Py), 91.31 (═C), 54.40 (O−CH_3), 28.15 (^{i}Pr CH), 24.91, 23.18, (^{i}Pr CH_3), −6.82 ($NiCH_3$). Anal. Calcd for $C_{28}H_{34}N_2NiO_2$: C, 68.73; H, 7.00; N, 5.73. Found: C, 68.71; H, 7.04; N, 5.68.

[(2,6-^{i}Pr$_2$C$_6$H$_3$)N═CHCHC(p-F$_3$CPh)O]Ni(Py)(CH$_3$) ***(3g)***. Yield: 91%. ^{1}H NMR (300 MHz, C_6D_6): δ 8.67 (d, $^3J_{HH}$ = 5.1 Hz, 2H, *o*-H Py), 7.59, 7.31 (d, 2H, *J* = 8.1 Hz, Ar H), 7.25−7.14 (m, 3H, Ar H), 6.69 (t, $^3J_{HH}$ = 7.8 Hz, 1H, *p*-H Py), 6.31 (d, 2H, *J* = 8.7 Hz, Ar H), 6.31 (t, $^3J_{HH}$ = 6.9 Hz, *m*-H Py), 5.76 (d, $^3J_{HH}$ = 6.3 Hz, 1H, C═C−H), 4.44 (sept, $^3J_{HH}$ = 6.9 Hz, 2H, ^{i}Pr CH), 1.65, 1.33, (d, $^3J_{HH}$ = 6.9 Hz, 12H, ^{i}Pr CH_3), −0.46 (s, 3H, $NiCH_3$). ^{13}C NMR (600 MHz, C_6D_6): δ 170.50 (NC), 160.47, 151.57, 141.83, 135.51, 128.04, 126.59, 125.88, 124.91, 124.45, 124.05, 123.28, 122.95 (Ar, Py), 92.79 (═C), 28.18 (^{i}Pr CH), 24.84, 23.09 (^{i}Pr CH_3), −6.47 ($NiCH_3$). Anal. Calcd for $C_{28}H_{31}F_3N_2NiO$: C, 63.78; H, 5.93; N, 5.31. Found: C, 63.73; H, 5.96; N, 5.33.

Synthesis of Complexes 4a−d. A solution of ligand **2a** (0.29 g, 1.0 mmol) in THF (15 mL) was added to sodium hydride (48 mg, 2.0 mmol). Immediately a large amount of bubbles were emitted from the mixture and a yellow solution formed. Then the solution was stirred at room temperature for 4 h, filtered, and evaporated. The solid residue was washed with hexane (20 mL) and dried under vacuum, affording a light yellow sodium salt. The sodium salt was dissolved in toluene at room temperature and transferred to a toluene solution of *trans*-$PhNi(PPh_3)_2Cl$ (0.7 g, 1.0 mmol) in a Schlenk flask with stirring at room temperature for 12 h, forming a red solution. Then the reaction mixture was filtered by cannula filtration and the filtrate was concentrated in vacuo to about 4 mL, to which hexane (15 mL) was added. Subsequently, yellow crystals precipitated from the solution, which were isolated via filtration and washed several times with cold hexane to yield 0.41 g (60%) of complex **4a**. The other neutral nickel(II) complexes **4b−d** were prepared by the same procedure in similar yields.

[(2,6-^{i}Pr$_2$C$_6$H$_3$)N═CHCHC(^{t}Bu)O]Ni(Ph)(PPh$_3$) ***(4a)***. ^{1}H NMR (300 MHz, C_6D_6): δ 7.79−7.65 (m, 6H, Ar H), 7.05−6.89 (m, 15H, Ar H), 6.36−6.25 (m, 3H, Ar H), 5.35 (d, $^3J_{HH}$ = 6.6 Hz, 1H, C═CH), 4.26 (sept, $^3J_{HH}$ = 6.9 Hz, 2H, ^{i}Pr CH), 1.32, 1.21 (d, $^3J_{HH}$ = 6.9 Hz, 12H, ^{i}Pr CH_3), 0.80 (9H, ^{t}Bu H). ^{13}C NMR (300 MHz, C_6D_6): δ 187.32 (NC), 160.46, 151.07, 141.77, 137.37, 134.84, 134.47, 134.40, 132.15, 129.50, 129.33, 125.21, 125.08, 122.44, 120.99 (Ar), 89.62 (═C), 39.12 (^{t}Bu C), 28.66 (^{t}Bu CH_3), 28.19 (^{i}Pr CH), 25.73, 22.72 (^{i}Pr CH_3). Anal. Calcd for $C_{43}H_{48}NNiOP$: C, 75.45; H, 7.07; N, 2.05. Found: C, 75.42; H, 7.10; N, 2.08.

[(2,6-^{i}Pr$_2$C$_6$H$_3$)N═CHCHC(Ph)O]Ni(Ph)(PPh$_3$) ***(4b)***. The synthesis of the complex has been reported in our previous work.[20c]

[(2,6-^{i}Pr$_2$C$_6$H$_3$)N═CHCHC(1-naphthyl)O]Ni(Ph)(PPh$_3$) ***(4c)***. Yield: 63%. ^{1}H NMR (300 MHz, C_6D_6): δ 8.34 (d, $^3J_{HH}$ = 8.4 Hz, 1H, N═CH), 7.63−7.39 (m, 9H, Ar H), 7.17−6.79 (m, 18H, Ar H), 6.40−6.30 (m, 3H, Ar H), 5.69 (d, $^3J_{HH}$ = 6.3 Hz, 1H, C═CH), 4.36 (sept, $^3J_{HH}$ = 6.9 Hz, 2H, ^{i}Pr CH), 1.39, 1.27 (d, $^3J_{HH}$ = 6.9 Hz, 12H, ^{i}Pr CH_3). ^{13}C NMR (300 MHz, C_6D_6): δ 175.53 (NC), 160.31, 150.87, 146.89, 146.57, 141.43, 139.50, 137.70, 134.22, 134.15, 133.65, 131.59, 131.31, 130.42, 129.18, 128.50, 126.59, 125.47, 125.26, 125.08, 125.04, 124.57, 122.37, 121.14 (Ar), 97.18 (═C), 28.65 (^{i}Pr CH), 25.71, 22.62 (^{i}Pr CH_3). Anal. Calcd for $C_{49}H_{46}NNiOP$: C, 78.00; H, 6.14; N, 1.86. Found: C, 78.02; H, 6.11; N, 1.85.

[(2,6-^{i}Pr$_2$C$_6$H$_3$)N═CHCHC(9-anthryl)O]Ni(Ph)(PPh$_3$) ***(4d)***. Yield: 58%. ^{1}H NMR (300 MHz, C_6D_6): δ 8.33 (d, $^3J_{HH}$ = 8.7 Hz, 2H, Ar H), 7.99 (s, 1H, Ar H), 7.71 (d, $^3J_{HH}$ = 8.1 Hz, 2H, Ar H), 7.53−7.19 (m, 11H, Ar H), 7.13−6.89 (m, 5H, Ar H), 6.81−6.70 (m, 9H, Ar H), 6.44−6.35 (m, 3H, Ar H), 5.55 (d, $^3J_{HH}$ = 6.3 Hz, 1H, C═C−H), 4.51 (sept, $^3J_{HH}$ = 6.9 Hz, 2H, ^{i}Pr CH), 1.39, 1.32 (d, $^3J_{HH}$ = 6.9 Hz, 12H, ^{i}Pr CH_3). ^{13}C NMR (300 MHz, C_6D_6): δ 175.64 (NC), 160.44, 150.99, 147.03, 146.71, 141.55, 139.62, 137.82, 134.34, 134.27, 131.71, 131.43, 129.30, 128.62, 126.71, 125.59, 125.38, 125.20, 125.16, 124.69, 122.49, 121.26 (Ar), 97.30 (═C), 28.77 (^{i}Pr CH), 25.83, 22.74 (^{i}Pr CH_3). Anal. Calcd for $C_{53}H_{48}NNiOP$: C, 79.11; H, 6.01; N, 1.74. Found: C, 79.13; H, 5.98; N, 1.71.

Ethylene Polymerization. A 200 mL autoclave was heated under vacuum up to 130 °C for 10 h and then was cooled to the desired reaction temperature in an oil bath with constant temperature. The vessel was purged three times with ethylene and then was charged with toluene (50 mL) under vacuum. A 10 or 20 μmol amount of cocatalyst dissolved in 10 mL of toluene was added into the autoclave by syringe if necessary, followed by the same amount of catalyst. The total volume of the reaction medium was fixed at 100 mL. The reactor was then sealed and pressurized to the desired level, and the stirring motor was engaged. Temperature control was maintained by internal cooling water coils with temperature increases within 2 °C in every case. After the prescribed reaction time, the stirring motor was stopped, the reactor was vented, and the polymer was isolated via precipitation from ethanol. The solid polyethylene was filtered, washed with acetone several times, and dried at 60 °C for more than 10 h under vacuum.

Crystallographic Studies. Crystals for X-ray analysis were obtained as described in the preparations. The crystallographic data, collection parameters, and refinement parameters are given in Table 1. The crystals were manipulated in a glovebox. The intensity data were collected with the ω scan mode (186 K) on a Bruker Smart APEX diffractometer with CCD detector using Mo Kα radiation (λ = 0.710 73 Å). Lorentz−polarization factors were used for the intensity data, and absorption corrections were performed using the SADABS program. The crystal structures were solved using the SHELXTL program and refined using full-matrix least squares. The positions of hydrogen atoms were calculated theoretically and included in the final cycles of refinement in a riding model along with attached carbons.

■ ASSOCIATED CONTENT

Ⓢ Supporting Information

CIF files giving X-ray data for the crystal structure determinations. This material is available free of charge via the Internet at http://pubs.acs.org.

■ AUTHOR INFORMATION

Corresponding Author

*Fax: +86-431-85262039. E-mail: ysli@ciac.jl.cn.

■ ACKNOWLEDGMENTS

We are grateful for a subsidy provided by the National Natural Science Foundation of China (No. 20923003).

■ REFERENCES

(1) (a) Johnson, L. K.; Killian, C. M.; Brookhart, M. *J. Am. Chem. Soc.* **1995**, *117*, 6414−6415. (b) Ittel, S. D.; Johnson, L. K.; Brookhart, M. *Chem. Rev.* **2000**, *100*, 1169−1203. (c) Nakamura, A.; Ito, S.; Nozaki, K. *Chem. Rev.* **2009**, *109*, 5215−5244. (d) Makio, H.; Terao, H.; Iwashita, A.; Fujita, T. *Chem. Rev.* **2011**, *111*, 2363−2449. (e) Delferro, M.; Marks, T. J. *Chem. Rev.* **2011**, *111*, 2450−2485. (f) Takeuchi, D. *Dalton Trans.* **2010**, *39*, 311−328.

(2) (a) Johnson, L. K.; Mecking, S.; Brookhart, M. *J. Am. Chem. Soc.* **1996**, *118*, 267−268. (b) Mecking, S.; Johnson, L. K.; Wang, L.; Brookhart, M. *J. Am. Chem. Soc.* **1998**, *120*, 888−899. (c) Li, W.; Zhang, X.; Meetsma, A.; Hessen, B. *J. Am. Chem. Soc.* **2004**, *126*, 12246−12247.

(3) (a) Popeney, C.; Guan, Z. B. *Organometallics* **2005**, *24*, 1145−1155. (d) Camachoa, D. H.; Guan, Z. B. *Chem. Commun.* **2010**, *46*, 7879−7893.
(4) (a) Burns, C. T.; Jordan, R. F. *Organometallics* **2007**, *26*, 6737−6749. (b) Chen, C.; Luo, S.; Jordan, R. F. *J. Am. Chem. Soc.* **2008**, *130*, 12892−12893. (c) Chen, C.; Luo, S.; Jordan, R. F. *J. Am. Chem. Soc.* **2010**, *132*, 5273−5284.
(5) (a) Kermagoret, A.; Braunstein, P. *Organometallics* **2008**, *27*, 88−99. (b) Chavez, P.; Braunstein, P. *Organometallics* **2009**, *28*, 1776−1784. (c) Kermagoret, A.; Braunstein, P. *Dalton Trans.* **2008**, *37*, 1564−1573.
(6) (a) Rose, G. M.; Coates, G. W. *J. Am. Chem. Soc.* **2006**, *128*, 4186−4187. (b) Rose, G. M.; Coates, G. W. *Macromolecules* **2008**, *41*, 9548−9555. (c) Okada, T.; Takeuchi, D.; Shishido, A.; Ikeda, T.; Osakada, K. *J. Am. Chem. Soc.* **2009**, *131*, 10852−10853.
(7) (a) Wang, H. Y.; Meng, X.; Jin, G. X. *Dalton Trans.* **2006**, *35*, 2579−2585. (b) Huang, Y. B.; Jin, G. X. *Organometallics* **2008**, *27*, 259−269. (c) Ceder, R. M.; Muller, G.; Ordinas, M.; Ordinas, J. I. *Dalton Trans.* **2007**, *36*, 83−90. (d) Han, F. B.; Sun, X. L.; Tang, Y. *Organometallics* **2008**, *27*, 1924−1928. (e) Gao, R.; Sun, W. H. *Organometallics* **2008**, *27*, 5641−5648. (f) Brasse, M.; Campora, J. *Organometallics* **2008**, *27*, 4711−4723. (g) Dorcier, A.; Basset, J. M. *Organometallics* **2009**, *28*, 2173−2178. (h) Liu, F. S.; Gao, H. Y.; Wu, Q. *Macromolecules* **2009**, *42*, 7789−7796. (i) Noda, S.; Nozaki, K. *Organometallics* **2009**, *28*, 656−658. (j) Zai, S. B.; Wu, Q. *Chem. Commun.* **2010**, *46*, 4321−4323. (k) Sachse, A.; Demeshko, S.; Dechert, S.; Daebel, V.; Lange, A.; Meyer, F. *Dalton Trans.* **2010**, *39*, 3903−3914.
(8) (a) Drent, E.; van Dijk, R.; van Ginkel, R.; van Oort, B.; Pugh, R. I. *Chem. Commun.* **2002**, *46*, 744−745. (b) Kochi, T.; Yoshimura, K.; Nozaki, K. *Dalton Trans.* **2006**, *35*, 25−27.
(9) See the following reviews and references therein: (a) Berkefeld, A.; Mecking, S. *Angew. Chem., Int. Ed.* **2008**, *47*, 2538−2542. (b) Kageyama, T.; Ito, S.; Nozaki, K. *Asian J. Chem.* **2011**, *6*, 690−697.
(10) Keim, W.; Kowaldt, F. H.; Goddard, R.; Krüger, C. *Angew. Chem., Int. Ed.* **1978**, *17*, 466−467.
(11) (a) Wang, C.; Friedrich, S.; Younkin, T. R.; Li, R. T.; Grubbs, R. H.; Bansleben, D. A.; Day, M. W. *Organometallics* **1998**, *17*, 3149−3151. (b) Younkin, T. R.; Connor, E. F.; Henderson, J. I.; Friedrich, S. K.; Grubbs, R. H.; Bansleben, D. A. *Science* **2000**, *287*, 460−462.
(12) (a) Zuideveld, M.; Wehrmann, P.; Röhr, C.; Mecking, S. *Angew. Chem., Int. Ed.* **2004**, *43*, 869−873. (b) Kuhn, P.; Sémeril, D.; Jeunesse, C.; Matt, D.; Neuburger, M.; Mota, A. *Chem. Eur. J.* **2006**, *12*, 5210−5219. (c) Göttker-Schnetmann, I.; Wehrmann, P.; Röhr, C.; Mecking, S. *Organometallics* **2007**, *26*, 2348−2362. (d) Bastero, A.; Göttker-Schnetmann, I.; Röhr, C.; Mecking, S. *Adv. Synth. Catal.* **2007**, *349*, 2307−2316. (e) Berkefeld, A.; Mecking, S. *J. Am. Chem. Soc.* **2009**, *131*, 1565−1574.
(13) (a) Kolb, L.; Monteil, V.; Mecking, S. *Angew. Chem., Int. Ed.* **2005**, *44*, 429−432. (b) Guironnet, D.; Friedberger, T.; Mecking, S. *Dalton Trans.* **2009**, *38*, 8929−8934. (c) Wehrmann, P.; Zuideveld, M. A.; Thomann, R.; Mecking, S. *Macromolecules* **2006**, *39*, 5995−6002. (d) Göttker-Schnetmann, I.; Korthals, B.; Mecking, S. *J. Am. Chem. Soc.* **2006**, *128*, 7708−7709. (e) Weber, C. H. M.; Chiche, A.; Krausch, G.; Rosenfeldt, S.; Ballauf, M.; Harnau, L.; Göttker-Schnetmann, I.; Tong, Q.; Mecking, S. *Nano Lett.* **2007**, *7*, 2024−2029.
(14) (a) Hu, T.; Tang, L. M.; Li, X. F.; Li, Y. S.; Hu, N. H. *Organometallics* **2005**, *24*, 2628−2632. (b) Hu, T.; Li, Y. G.; Liu, J. Y.; Li, Y. S. *Organometallics* **2007**, *26*, 2609−2615. (c) Mu, H. L.; Ye, W. P.; Song, D. P.; Li, Y. S. *Organometallics* **2010**, *29*, 6282−6290. (d) Song, D. P.; Li, Y. G.; Lu, R.; Hu, N. H.; Li, Y. S. *Appl. Organomet. Chem.* **2008**, *22*, 333−340.
(15) (a) Rodriguez, B. A.; Delferro, M.; Marks, T. J. *Organometallics* **2008**, *27*, 2166−2168. (b) Rodriguez, B. A.; Delferro, M.; Marks, T. J. *J. Am. Chem. Soc.* **2009**, *131*, 5902−5919.
(16) (a) Sujith, S.; Dae, J. J.; Na, S. J.; Park, Y.-W.; Choi, J. H.; Lee, B. Y. *Macromolecules* **2005**, *38*, 10027−10033. (b) Na, S. J.; Lee, B. Y. *J. Organomet. Chem.* **2006**, *691*, 611−620. (c) Zeller, A.; Strassner, T. *J. Organomet. Chem.* **2006**, *691*, 4379−4385. (d) Okada, M.; Shiono, T. *J. Organomet. Chem.* **2007**, *692*, 5183−5189. (e) Chen, Q.; Yu, J.; Huang, J. *Organometallics* **2007**, *26*, 617−625. (f) Wei, W. P.; Huang, B. T. *Inorg. Chem. Commun.* **2008**, *11*, 487−491. (g) Shen, M.; Sun, W. H. *J. Organomet. Chem.* **2008**, *693*, 1683−1695. (h) Li, W. F.; Sun, H. M.; Shen, Q. *J. Organomet. Chem.* **2008**, *693*, 2047−2051. (i) Chandran, D.; Kim, I. *J. Organomet. Chem.* **2009**, *694*, 1254−1258.
(17) (a) Boardman, B. M.; Bazan, G. C. *Acc. Chem. Res.* **2009**, *42*, 1579−1606. (b) Coffin, R. C.; Schneider, Y.; Kramer, E. J.; Bazan, G. C. *J. Am. Chem. Soc.* **2010**, *132*, 13869−13878.
(18) (a) Hicks, F. A.; Brookhart, M. *Organometallics* **2001**, *20*, 3217−3219. (b) Jenkins, J. C.; Brookhart, M. *Organometallics* **2003**, *22*, 250−256. (c) Hicks, F. A.; Jenkins, J. C.; Brookhart, M. *Organometallics* **2003**, *22*, 3533−3545. (d) Jenkins, J. C.; Brookhart, M. *J. Am. Chem. Soc.* **2004**, *126*, 5827−5842.
(19) (a) Zhang, L.; Brookhart, M.; White, P. S. *Organometallics* **2006**, *25*, 1868−1874. (b) Yu, S. M.; Mecking, S. *Macromolecules* **2007**, *40*, 421−428.
(20) (a) Li, X. F.; Li, Y. G.; Li, Y. S.; Chen, Y. X.; Hu, N. H. *Organometallics* **2005**, *24*, 2502−2510. (b) Song, D. P.; Ye, W. P.; Wang, Y. X.; Liu, J. Y.; Li, Y. S. *Organometallics* **2009**, *28*, 5697−5704. (c) Song, D. P.; Wu, J. Q.; Ye, W. P.; Mu, H. L.; Li, Y. S. *Organometallics* **2010**, *29*, 2306−2314. (d) Song, D. P.; Wang, Y. X.; Mu, H. L.; Li, B. X.; Li, Y. S. *Organometallics* **2011**, *30*, 925−934.
(21) Hansch, C.; Leo, A.; Taft, R. W. *Chem. Rev.* **199l**, *97*, 165−195.
(22) We employed density functional theory (DFT) calculations by using the Amsterdam Density Functional (ADF) program package.[26] A triple-STO basis set was employed for Ni, while all other atoms were described by a double-ζ plus polarization STO basis. The 1s electrons of the C, N and O atoms, as well as the 1s−2p electrons of the Ni atom, were treated as a frozen core.
(23) (a) Braunstein, P.; Chauvin, Y.; Mercier, S.; Saussine, L.; De Cian, A.; Fischer, J. *J. Chem. Soc., Chem. Commun.* **1994**, 2203−2204. (b) Soula, R.; Broyer, J. P.; Llauro, M. F.; Tomov, A.; Spitz, R.; Claverie, J.; Drujon, X.; Malinge, J.; Saudemont, T. *Macromolecules* **2001**, *34*, 2438−2442.
(24) (a) Gates, D. P.; Svejda, S. A.; Oñate, E.; Killian, C. M.; Johnson, L. K.; White, P. S.; Brookhart, M. *Macromolecules* **2000**, *33*, 2320−2334. (b) Galland, G. B.; Souza, R. F.; Mauler, R. S.; Nunes, F. F. *Macromolecules* **1999**, *32*, 1620−1925.
(25) (a) Hidai, M.; Kashiwagi, T.; Ikeuchi, T.; Uchida, Y. *J. Organomet. Chem.* **1971**, *30*, 279−282. (b) Campora, J.; Conejo, M. M.; Mereiter, K.; Palma, P. *J. Organomet. Chem.* **2003**, *683*, 220−239.
(26) (a) Baerends, E. J.; Ellis, D. E.; Ros, P. *Chem. Phys.* **1973**, *2*, 41−51. (b) Baerends, E. J.; Ros, P. *Chem. Phys.* **1973**, *2*, 52−59. (c) te Velde, G.; Baerends, E. J. *J. Comput. Phys.* **1992**, *99*, 8498−8503. (d) Fonseca, C. G.; Visser, O.; Snijders, J. G.; te Velde, G.; Baerends, E. J. In *Methods and Techniques in Computational Chemistry*; METECC-95; Clementi, E., Corongiu, G., Eds.; STEF: Cagliari, Italy, 1995; p 305.